

## Percolation on a multifractal scale-free planar stochastic lattice and its universality class

M. K. Hassan and M. M. Rahman

*Department of Physics, University of Dhaka, Dhaka 1000, Bangladesh*

(Received 19 April 2015; revised manuscript received 19 June 2015; published 6 October 2015)

We investigate site percolation on a weighted planar stochastic lattice (WPSL), which is a multifractal and whose dual is a scale-free network. Percolation is typically characterized by a threshold value  $p_c$  at which a transition occurs and by a set of critical exponents  $\beta$ ,  $\gamma$ ,  $\nu$  which describe the critical behavior of the percolation probability  $P(p)$ , mean cluster size  $S(p)$ , and the correlation length  $\xi$ . Besides, the exponent  $\tau$  characterizes the cluster size distribution function  $n_s(p_c)$  and the fractal dimension  $d_f$  characterizes the spanning cluster. We numerically obtain the value of  $p_c$  and of all the exponents. These results suggest that the percolation on WPSL belong to a separate universality class than on all other planar lattices.

DOI: [10.1103/PhysRevE.92.040101](https://doi.org/10.1103/PhysRevE.92.040101)

PACS number(s): 64.60.Ht, 61.43.Hv, 68.03.Fg, 82.70.Dd

Percolation is perhaps one of the most studied problems in statistical physics because it provides a general framework of statistical theories that deal with structural and transport properties in porous or heterogeneous media [1,2]. To study percolation one has to first choose a skeleton, namely, an empty lattice or a graph. Each site or bond of the lattice or graph is then either occupied with probability  $p$  or remains empty with probability  $1 - p$ , independent of the state of its neighbors. For small values of  $p$  we see mostly single or a few contiguous occupied sites, which are called clusters. As  $p$  increases, the mean cluster size always keeps growing at an increasingly faster rate until it comes to a state when suddenly a macroscopic cluster appears for the first time, spanning from one end of the lattice to its opposite end. This sudden onset of a spanning cluster in an infinite system occurs at a particular value of  $p$  known as the percolation threshold  $p_c$ . This is accompanied by a sudden or abrupt change in the behavior of the observable quantities with a small change in its control parameter  $p$ . Such a change is almost always found to be the signature of a phase transition that occurs in a wide range of phenomena [3,4]. This is why scientists in general and physicists in particular find percolation theory so attractive. Indeed, insight into the percolation problem facilitates the understanding of the phase transition and critical phenomena that lie at the heart of the modern development of statistical physics (see Ref. [5], which is an excellent review published recently).

Percolation on disordered lattices is potentially of great interest since many real-life phenomena deal with such disordered systems [6]. In recent decades there has been a surge of research activities in studying percolation on random and scale-free networks because the coordination number disorder of these networks is closely tied to many natural and man-made skeletons or media through which percolation occurs. For instance, infectious diseases, computer viruses, opinion, rumors, etc., usually spread through networks [7–12]. Besides, the flow of fluids usually takes place through a porous medium or through rocks, and hence the architecture of the skeleton is anything but regular [13]. In fact, the transport of fluid through multifractal porous media such as sedimentary strata and in oil reservoirs is of great interest in geological systems [14]. In this Rapid Communication, we investigate percolation on a weighted planar stochastic lattice (WPSL). One of us has recently shown that its coordination number distribution

follows a power law and its size distribution can be best described as multifractal [15]. In contrast, scale-free networks too have a power-law coordination number distribution, but nodes or sites in the scale-free networks are neither embedded on spatial positions nor have edges or surfaces. Our goal is to find how the two aspects, multifractality and power-law coordination number distributions, leave their signature in the percolation processes. Note that most of the studies on percolation have been restricted to the use of lattices with fixed coordination numbers, such as a square lattice, triangular lattice, honeycomb, etc. However, percolation on random or multifractal planar lattices in which the coordination number is not fixed has been of relatively recent interest [16,17]. The most interesting result of all these studies is that the critical exponents are independent of the details of the lattice structure and of the type of percolation (bond or site), but depend on the dimension of the lattice only [18]. That is, percolation on all lattices belongs to the same universality class if its embedding dimension  $d$  is the same. This is, however, no longer the case as we report that the percolation on all known planar lattices ( $d = 2$ ) belongs to one universality class and the percolation on WPSL belongs to another class.

The construction process of the WPSL (see Fig. 1) starts with an initiator, say, a square of unit area. The generator is then defined as the one that divides the initiator randomly into four smaller blocks. Thereafter, at each step, the generator is applied to only one block by picking it preferentially with respect to areas (see Ref. [15] for details of the construction process). This process ensures that the blocks with a greater area are more likely to be picked. We define each step of the division process as one time unit. The sum of the area of all the blocks of the WPSL always remains the same, although the number of blocks  $N$  grow with time  $t$ . It implies that  $N$  increases at the expense of the mean size of the blocks. Indeed, the mean cell area decreases with  $N$  as  $\langle a \rangle \sim N^{-1}$  or with  $t$  as  $\langle a \rangle \sim t^{-1}$  since  $\langle a \rangle = a/N$ , where the total area  $a$  of all the blocks is always equal to one. We therefore need to emphasize two ideas here. First, we can define the size of the side  $L$  of the WPSL as  $t^{1/2}$  as we do for square lattice  $L = N^{1/2}$ . Second, to make the cells of the WPSL have the same size, in the statistical sense, as we increase  $N$ , we have to scale up the cell sizes by a factor of  $t$ . We just need to multiply each quantity we measure by a factor  $t$  to compensate for the decreasing size of the blocks.

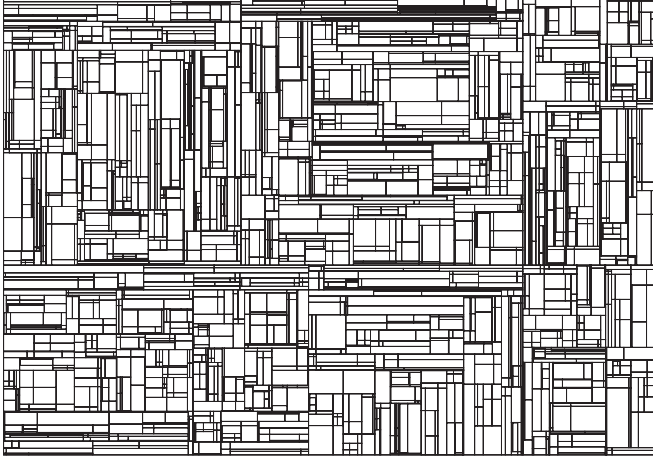


FIG. 1. A snapshot of the weighted stochastic lattice.

The construction process of WPSL might be simple but its various properties are far from that. First, it evolves by following several nontrivial conservation laws, namely, that the value of the quantity  $\sum_i^N x_i^{n-1} y_i^{4/n-1}$  is independent of time or size of the lattice  $\forall n$ , where  $x_i$  and  $y_i$  are the length and width of the  $i$ th block. Second, its dual, obtained by replacing each block with a node at its center and common border between blocks with an edge joining the two vertices, emerges as a scale-free network [15]. Third, if one considers that the  $i$ th block is populated with probability  $p_i \sim x_i^3$  or  $y_i^3$ , then the  $q$ th moment of  $p_i$  can be shown to exhibit the power law  $Z_q(\delta) \sim \delta^{-\tau(q)}$ , where  $\delta$  is the square root of the mean block area and

$$\tau(q) = \sqrt{9q^2 + 16} - (3q + 2). \quad (1)$$

Note that  $\tau(0) = 2$  is the dimension of the WPSL and  $\tau(1) = 0$  follows from the normalization of the probabilities  $\sum p_i = 1$  [19]. The Legendre transform of  $\tau(q)$ , on the other hand, gives the multifractal spectrum  $f(\alpha)$ , where the exponent  $\alpha$  is the negative derivative of  $\tau(q)$  with respect to  $q$ . Yet another feature of the WPSL is that it emerges through evolution and the area size distribution function of its cells exhibits dynamic scaling [20].

To study percolation on the WPSL we employ the Ziff-Newman algorithm [21] in which all the labeled sites or cells  $i = 1, 2, 3, \dots, (1 + 3t)$  are first randomized and arranged in an order in which the sites will be occupied. This algorithm allows us to create percolation states consisting of  $n + 1$  occupied sites simply by occupying one more site to its immediate past percolation state consisting of  $n$  occupied sites. We keep track of the number of clusters and their sizes as a function of  $n$  with regard to the occupation probability  $p = n/(1 + 3t)$ . In fact, the product of the number of occupied sites  $n$  and the mean area  $1/(1 + 3t)$  is equal to the mean area of all the occupied sites  $\langle a(n) \rangle$ , which is equal to 1 when all the sites are occupied, i.e., when  $n = N$ . In our simulation we use the periodic boundary condition whereby the lattice is viewed as a torus without an edge or surface.

In percolation, one of the primary objectives is to find the occupation probability  $p_c$  at which a cluster of contiguous occupied sites span the entire lattice, either horizontally

or vertically, for the first time. Of course, the occupation probability at which it occurs at each independent realization on a finite-size lattice will not be the same. In reality, we can get spanning even at very much less than  $p_c$  or not get it even at a much higher  $p$  than  $p_c$ . This is exactly why the percolation theory is a part of statistical physics. One way of dealing with this is to use the idea of spanning probability  $W(p)$  [22]. Consider that we have performed  $m$  independent realizations, and for each realization we check exactly at what value of  $p = n/N$  a cluster appears that connects the two opposite ends either horizontally or vertically, whichever comes first. The spanning probability  $W(p)$  is obtained by finding the relative frequency of occurrence of spanning cluster out of  $m$  independent realizations at  $p$ . The plot in Fig. 2(a) shows  $W(p)$  as a function of  $p$  for three different lattice sizes. Interestingly, all three plots meet at one particular point. It has a special significance as it is actually the percolation threshold  $p_c = 0.5265$  for the WPSL.

A careful look at the plots of  $W(p)$  vs  $p$  reveals that a given fixed value of  $W$  is obtained at an increasingly higher value of  $p$  for  $p < p_c$  as we increase  $L$ , which is indicated by the arrow in Fig. 2 (a). To quantify this, we draw a horizontal line, for instance, at  $W(p) = 0.3$ , and a vertical line at  $p_c = 0.5265$ . The horizontal line intersects all three curves and the vertical line for different  $L$ , say, at  $A, B, C$ , and at  $O$ . The distance  $OA, OB, OC$ , etc., thus represents  $(p_c - p)$ . In the inset of Fig. 2(a) we plot  $\log(p_c - p)$  vs  $\log(L)$ , and a linear fit to the points gives a perfect straight line with a slope  $1/\nu = 0.6112(38)$ , and hence we can write

$$(p_c - p) \sim L^{-1/\nu}. \quad (2)$$

We thus find that  $\nu = 1.636(10)$  for WPSL, which is significantly different from the known value  $\nu = 4/3$  for all the regular planar lattices. The relation given by Eq. (2) implies that  $(p_c - p)L^{1/\nu}$  is a dimensionless quantity in the sense that for a given value of  $W$ , the value of  $(p_c - p) \rightarrow 0$  as  $L \rightarrow \infty$  such that the numerical value of  $(p_c - p)L^{1/\nu}$  remains invariant regardless of the lattice size  $L$ . We now plot  $W(p)$  as a function of  $(p_c - p)L^{1/\nu}$  [see Fig. 2(b)], and find that all the distinct curves of Fig. 2(a) collapse onto a single universal curve. It implies that

$$W(p) \sim L^\eta \phi((p_c - p)L^{1/\nu}), \quad (3)$$

with exponent  $\eta = 0$ , where  $\phi$  is the scaling function [23]. It states that the spanning probability  $W$  itself is a dimensionless quantity and for infinite lattice sizes it would become like a step function around  $p_c$  [24].

The fact is that not all the occupied sites belong to the spanning cluster. To this end, we define the percolation probability  $P$  as the ratio of the area of the spanning cluster  $A_{\text{span}}t$  to the total area of the lattice  $at$ , and hence  $P(p) = A_{\text{span}}$  since the total area of the lattice is always equal to one. Unlike  $W(p)$  vs  $p$ , the distinct curves of the  $P(p)$  vs  $p$  plots [see Fig. 3(a)] for different lattice sizes do not meet exactly at  $p_c$ , which we can only appreciate if we zoom in. Unlike the  $W(p)$  vs  $p$  case, if we apply the same rule to the  $P$  vs  $p$  case and plot  $P$  vs  $(p - p_c)L^{1/\nu}$ , we do not get a data collapse. Instead, we find that for a given value of  $(p - p_c)L^{1/\nu}$ , the  $P$  value decreases with lattice size  $L$ . To quantify the extent of the decrease, we measure the heights at a given value of

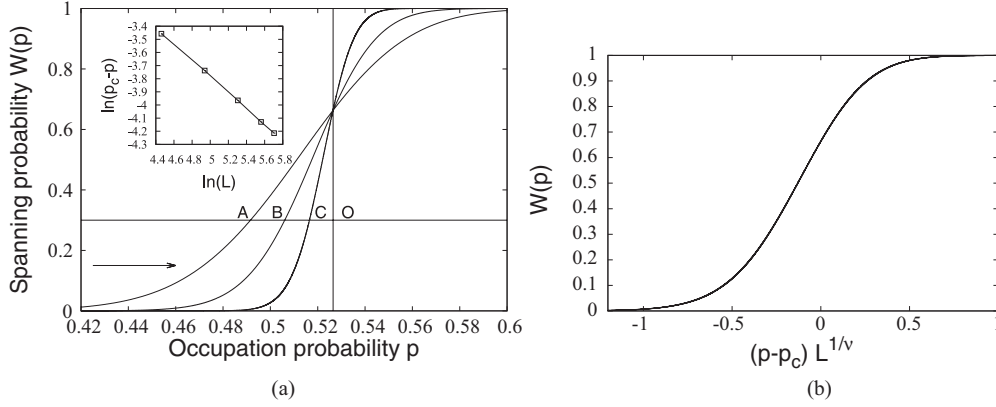


FIG. 2. (a) Plots of spanning probability  $W(p)$  vs  $p$  for different lattice sizes  $L = N^{1/2}$ , where  $N = 1 + 3t$  and  $t = 1000, 6500$ , and  $66\,667$ . The arrow points in the direction of increasing  $L$ . The inset shows a linear regression fit to the data points obtained by plotting  $\ln(p_c - p)$  vs  $\ln(L)$  with a slope  $1/\nu = 0.6112(38)$ , where each data point represents an average over 300 000 independent realizations. (b) Excellent data collapse confirms the correctness of our estimation of the exponent  $\nu$ .

$(p - p_c)L^{1/\nu}$  for different  $L$ . Plotting them in the log-log scale, we find a straight line [see the inset of Fig. 3(a)] with a slope  $\beta/\nu = 0.1357(5)$ , and hence we can write

$$P \sim L^{-\beta/\nu}. \quad (4)$$

It implies that if we now plot  $PL^{\beta/\nu}$  vs  $(p - p_c)L^{1/\nu}$ , all the distinct plots of  $P$  vs  $p$  should collapse into a single universal curve. Indeed, we find an excellent data collapse, as shown Fig. 3(b). This again implies that percolation probability  $P$  exhibits finite-size scaling,

$$P(p_c - p, L) \sim L^{-\beta/\nu} \phi((p - p_c)L^{1/\nu}). \quad (5)$$

Now, using Eq. (2) in Eq. (4) to eliminate  $L$  in favor of  $p - p_c$ , we get

$$P \sim (p - p_c)^\beta, \quad (6)$$

where  $\beta = 0.222(2)$  for WPSL, whereas  $\beta = 5/36$  for all known planar lattices.

Percolation is all about clusters, and hence the cluster size distribution function  $n_s(p)$  plays a central role in the

description of the percolation theory. It is defined as the number of clusters of size  $s$  per site. In terms of  $n_s(p)$  we can define  $f_s = sn_s(p) / \sum_{s=1}^{\infty} sn_s$  as the probability that the cluster to which an arbitrary occupied sites belongs is exactly of size  $s$ . The mean cluster size  $S(p)$  then is defined as

$$S(p) = \sum_s s f_s = \frac{\sum_s s^2 n_s}{\sum_s s n_s}, \quad (7)$$

where the sum is over the finite clusters only. In the case of percolation on the WPSL, we regard  $s$  as the cluster area. It is important to mention that each time we evaluate the ratio of the second and the first moment of  $n_s$ , we also have to multiply the result by  $t$ , the time at which the snapshot of the lattice is taken, to compensate for the decreasing block size with increasing block number  $N$ . The mean cluster size therefore is  $S = \frac{1}{p} \sum_s s^2 n_s t$ , where  $\sum_s s n_s = p$  is the sum of the areas of all the clusters. Note that the spanning cluster is excluded from both the sums of Eq. (7). In Fig. 4(a) we plot  $S(p)$  as a function of  $p$  for different lattice sizes  $L$ . We observe that there are two main effects as we increase the lattice size. First, we see

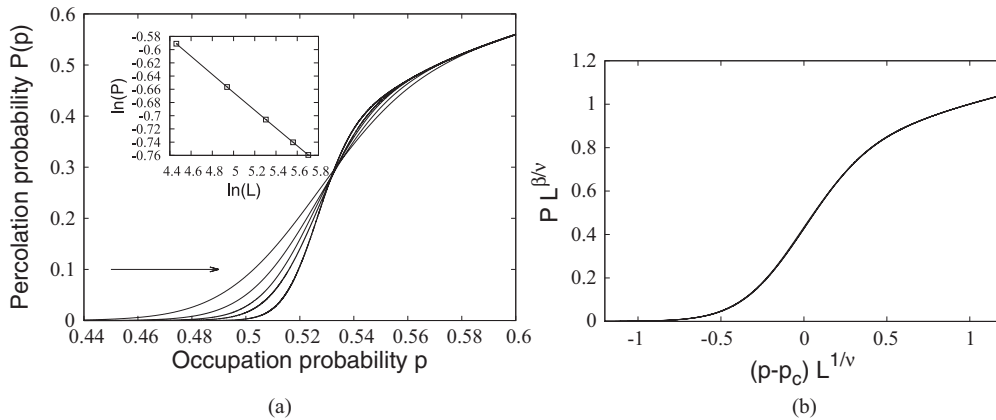


FIG. 3. (a) Plots of percolation probability  $P(p)$  vs  $p$  for different sizes  $L(t)$  where the arrow points in the direction of increasing  $L(t)$ , and  $t = 2500, 6500, 13\,500, 22\,534$ , and  $66\,667$ . Here, each data point represents an average over 300 000 independent realizations. The inset shows a plot of  $\ln(P)$  at a given value of  $(p - p_c)L^{1/\nu}$  vs  $\ln(L)$ . The linear regression fit gives an excellent straight line with a slope  $\beta/\nu = 0.1357(5)$ . (b) We plot  $PL^{\beta/\nu}$  vs  $(p - p_c)L^{1/\nu}$  instead of  $P$  vs  $p$  and find an excellent data-collapse which confirms that the estimates for the exponents  $\beta$  and  $\nu$  are correct.

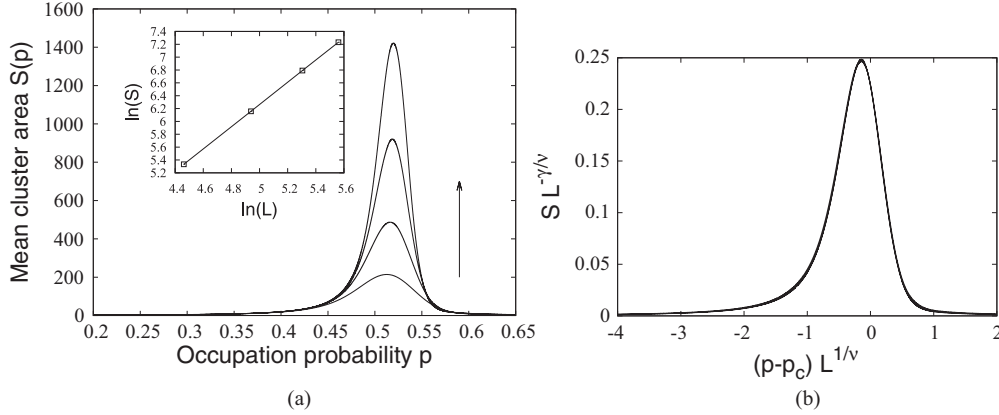


FIG. 4. (a) Mean cluster area  $S(p)$  vs  $p$  for different  $L$ . The arrow points in the direction of increasing  $L(t)$ , where  $t = 2500, 6500, 13\,500$ , and  $22\,534$ . Here, each data point represents an average over 200 000 independent realizations. The inset shows a plot of  $\ln(S)$  at a given value of  $(p - p_c)L^{1/\nu}$  vs  $\ln(L)$ . The linear regression yields an excellent straight line with a slope  $\gamma/\nu = 1.7281(19)$ . (b) We plot  $SL^{-\gamma/\nu}$  vs  $(p - p_c)L^{1/\nu}$  find that all distinct curves of (a) collapsed onto a single universal curve as expected according to finite-scaling hypothesis. It confirms that the estimates for the exponents  $\gamma$  and  $\nu$  are correct.

that the mean cluster area always increases as we increase the occupation probability. However, as the  $p$  value approaches to  $p_c$ , we find that the peak height grows profoundly with  $L$ .

The increase of the height at a given value of  $(p_c - p)L^{1/\nu}$  with a linear lattice size  $L$  can be quantified by plotting these heights versus  $L$  in the log-log scale, which gives a straight line [see the inset of Fig. 4(a)], revealing

$$S \sim L^{\gamma/\nu}, \quad (8)$$

where  $\gamma/\nu = 1.7281(19)$ . A careful observation reveals that there is also a shift in the  $p$  value at which the peaks occur. We find that the magnitude of this shift  $(p_c - p)$  becomes smaller with increasing  $L$  following a power law  $(p_c - p) \sim L^{-1/\nu}$ . Plotting the same data of Fig. 4(a) by measuring the mean cluster area  $S$  in units of  $L^b$  and  $(p_c - p)$  in units of  $L^{-1/\nu}$ , respectively, we find that all the distinct plots of  $S$  vs  $p$  collapse onto one universal curve [see Fig. 4(b)]. It again implies that the mean cluster area also exhibits finite-size scaling,

$$S \sim L^{\gamma/\nu} \phi((p_c - p)L^{1/\nu}). \quad (9)$$

Eliminating  $L$  from Eq. (8) in favor of  $(p_c - p)$  by using  $(p_c - p) \sim L^{-1/\nu}$ , we find that the mean cluster area diverges the following power law,

$$S \sim (p_c - p)^{-\gamma}, \quad (10)$$

with exponent  $\gamma = 2.827(20)$ . This is also significantly different from the known value  $\gamma \sim 2.389$  for all the regular planar lattices.

We can also obtain the exponent  $\tau$  by plotting the cluster area distribution function  $n_s(p)$  at  $p_c$ . In Fig. 5(a) we plot  $n_s(p_c)$  vs  $s$  in the log-log scale and find a straight line, except near the tail, where there is a hump due to the finite-size effect. However, we also observe that as the lattice size  $L$  increases, the extent of the straight line increases, too. It implies that if the size  $L$  was infinitely large we would have a perfect straight line obeying  $n_s(p_c) \sim s^{-\tau}$ . The slope of the straight line  $\tau = 2.0728(25)$ , which is a little more than the known value for planar lattices  $\tau = 187/91$ . We already know that the

mean cluster area  $S \rightarrow \infty$  as  $p \rightarrow p_c$ . According to Eq. (7),  $S$  can only diverge if its numerator diverges. Generally, we know that  $\sum_{s=1}^{\infty} s^\alpha$  converges if  $\alpha < -1$  and diverges if  $\alpha \geq -1$ . Applying it into both the numerator and the denominator of Eq. (7) at  $p_c$  gives a bound that  $2 < \tau < 3$ . Now, in the large  $s$  limit we postulate a scaling ansatz

$$n_s(p) \sim s^{-\tau} e^{-s/s_\xi}, \quad (11)$$

where  $s_\xi$  is the cutoff cluster size. Using the ansatz in Eq. (7), and taking the continuum limit we get

$$S \sim s_\xi^{3-\tau}. \quad (12)$$

We know that  $s_\xi$  diverges as  $(p_c - p)^{1/\sigma}$ , where  $\sigma = 1/(vd_f)$ , and hence comparing it with Eq. (10) we get

$$\tau = 3 - \gamma\sigma. \quad (13)$$

There exists another scaling relation  $\tau = 1 + d/d_f$  which can also be used to find the  $\tau$  value. However, to use these we need to know the fractal dimension  $d_f$  that quantifies the extent of ramification of the spanning cluster. The fractal dimension  $d_f$  quantifies the extent of ramification of the spanning cluster. It can be obtained by finding the gradient of the plot of the size of the spanning cluster  $M$  as a function of lattice size  $L$  in the log-log scale [see Fig. 5(b)]. We find  $d_f = 1.8642(19)$  and that for regular planar lattices  $d_f \sim$

TABLE I. The critical exponents for percolation in the WPSL and in the regular planar lattice are given alongside.

| Exponents | Regular 2D lattice | WPSL       |
|-----------|--------------------|------------|
| $\nu$     | 4/3                | 1.636(10)  |
| $\beta$   | 5/36               | 0.222(2)   |
| $\gamma$  | 43/18              | 2.827(20)  |
| $\tau$    | 187/91             | 2.0728(25) |
| $d_f$     | 91/48              | 1.8642(19) |

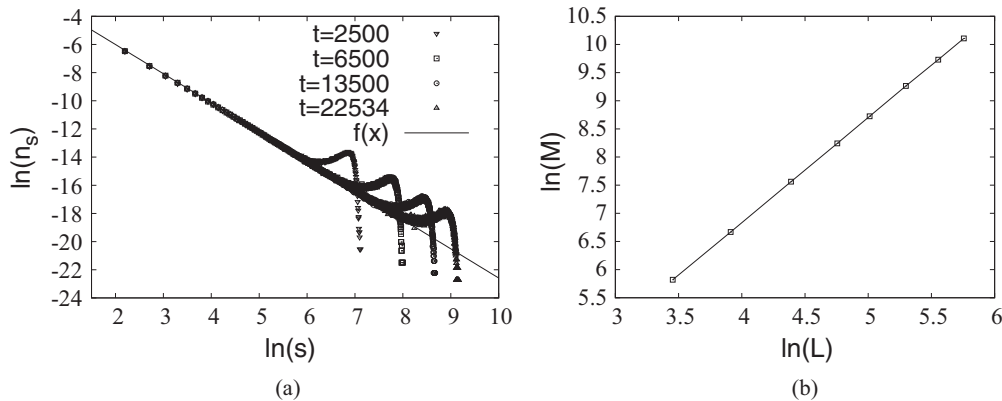


FIG. 5. (a) The plot of  $\log(n_s)$  vs  $\log(s)$  for different lattice sizes  $L = (1 + 3t)^{1/2}$ , where  $t = 2500, 6500, 13500$ , and  $22534$ . (b) The plot of  $\ln(M)$  vs  $\ln(L)$ . In either case, each data point represents an average over 100 000 independent realizations.

1.895. Note that a small difference in the fractal dimension makes a huge difference in the stringiness or in the extent of ramification of the object. Using the value  $d_f = 1.8642$  in the scaling relations gives 2.073 and 2.0728, which coincide up to two to three decimal places to the one obtained from Fig. 5(b). Besides the scaling relations for  $\tau$ , we also have scaling relations for  $\beta$  and  $\gamma$ , namely,  $\beta = \nu(d - d_f)$  and  $\gamma = \nu(2d_f - d)$ , which we can use for a consistency check. To this end, we find that our estimates for various exponents satisfy these relations up to quite a good extent. (See Table I.)

To summarize, we have studied site percolation on a scale-free multifractal planar lattice using extensive Monte Carlo simulations. We obtained the  $p_c$  value and the characteristic exponents  $\nu$ ,  $\beta$ ,  $\gamma$ ,  $\tau$ ,  $\sigma$ , and  $d_f$  which characterize the percolation transition. Note that it is the sudden onset of a spanning cluster at the threshold  $p_c$ , which is accompanied by a discontinuity or divergence of some the observable quantities, that makes the percolation transition a critical phenomenon. One of the most interesting and useful results of percolation

theory is that the values of the various exponents depend only on the dimensionality of the lattice as they are found to be independent of not only the type of lattice (e.g., hexagonal, triangular, or square, etc.) but also of the type of percolation (site or bond). This central property of percolation theory is known as universality. In 2004, Corso *et al.* performed percolation on a particular multifractal planar lattice whose coordination number distribution is, however, not scale-free as WPSL, and still they found that the exponents share the same universality class as for the planar regular lattices [17]. Thus, for WPSL it was expected that the  $p_c$  value would be different due to the unique nature of its coordination number distribution, but it was not expected to fall into a different universality class. It would be interesting to check the role of the exponents  $\gamma$  of the power-law coordination number distribution in the classification of universality classes. We intend to do so in our future endeavor.

One of us (M.K.H.) wishes to acknowledge helpful correspondence with R. M. Ziff.

- 
- [1] D. Stauffer and A. Aharony, *Introduction to Percolation Theory* (Taylor & Francis, London, 1994).
- [2] *Fractals and Disordered Systems*, edited by A. Bunde and S. Havlin (Springer, New York, 1996).
- [3] H. E. Stanley, *Introduction to Phase Transitions and Critical Phenomena* (Oxford University Press, New York 1971).
- [4] J. J. Binney, N. J. Dowrick, A. J. Fisher, and M. E. J. Newman, *The Theory of Critical Phenomena* (Oxford University Press, New York, 1992).
- [5] A. A. Saberi, *Phys. Rep.* **578**, 1 (2015).
- [6] M. Sahimi, *Applications of Percolation Theory* (Taylor & Francis, London, 1994).
- [7] M. E. J. Newman and D. J. Watts, *Phys. Rev. E* **60**, 7332 (1999).
- [8] C. Moore and M. E. J. Newman, *Phys. Rev. E* **62**, 7059 (2000).
- [9] R. Cohen, K. Erez, D. ben-Avraham, and S. Havlin, *Phys. Rev. Lett.* **85**, 4626 (2000).
- [10] S. Boccaletti, V. Latora, Y. Moreno, M. Chavez, and D.-U. Hwang, *Phys. Rep.* **424**, 175 (2006).
- [11] S. N. Dorogovtsev and J. F. F. Mendes, *Evolution of Networks* (Oxford University Press, Oxford, UK, 2003).
- [12] R. Pastor-Satorras and A. Vespignani, *Evolution and Structure of the Internet: A Statistical Physics Approach* (Cambridge University Press, Cambridge, UK, 2004).
- [13] H. Dashtian, G. R. Jafari, M. Sahimi, and M. Masihi, *Physica A* **390**, 2096 (2011).
- [14] P. N. Khue, O. Fluseby, A. Saucier, and J. Muller, *J. Phys.: Condens. Matter* **14**, 2347 (2002).
- [15] M. K. Hassan, M. Z. Hassan, and N. I. Pavel, *New J. Phys.* **12**, 093045 (2010); *J. Phys.: Conf. Ser.* **297**, 012010 (2011).
- [16] H.-P. Hsu and M.-C. Huang, *Phys. Rev. E* **60**, 6361 (1999).
- [17] G. Corso, J. E. Freitas, L. S. Lucena, and R. F. Soares, *Phys. Rev. E* **69**, 066135 (2004).
- [18] F. Yonezawa, S. Sakamoto, and M. Hori, *Phys. Rev. B* **40**, 636 (1989); **40**, 650 (1989).

- [19] J. Feder, *Fractals* (Plenum, New York, 1988).
- [20] F. R. Dayeen and M. K. Hassan, [arXiv:1409.7928v1](https://arxiv.org/abs/1409.7928v1) [cond-mat.stat-mech].
- [21] M. E. J. Newman and R. M. Ziff, *Phys. Rev. Lett.* **85**, 4104 (2000); *Phys. Rev. E* **64**, 016706 (2001).
- [22] R. M. Ziff, *Phys. Rev. Lett.* **69**, 2670 (1992).
- [23] A. A. Saberi, *Appl. Phys. Lett.* **97**, 154102 (2010).
- [24] G. I. Barenblatt, *Scaling, Self-Similarity, and Intermediate Asymptotics* (Cambridge University Press, Cambridge, UK, 1996).